Synthesis, Characterization and Nonlinear Optical Property of Graphene-C$_{60}$ Hybrid

Xiaoyan Zhang[1], ZhiBo Liu[2], Yi Huang[1], Xiangjian Wan[1],
Jianguo Tian[2], Yanfeng Ma[1], and Yongsheng Chen[1, *]

[1]*Key Laboratory of Functional Polymer Materials and Center for Nanoscale Science and Technology,
Institute of Polymer Chemistry, College of Chemistry, Nankai University, Tianjin 300071, China*
[2]*Key Laboratory of Weak Light Nonlinear Photonics, Ministry of Education, and Teda Applied Physics School,
Nankai University, Tianjin 300457, China*

The graphene-C$_{60}$ hybrid has been synthesized and characterized. Its nonlinear optical property was investigated. Raman spectroscopy suggested a strong interaction between C$_{60}$ and graphene. Based on UV and elemental analysis measurement, it is estimated that one C$_{60}$ molecule is covalently attached for every ∼110 carbon atoms in graphene. The nonlinear optical performance of this hybrid material was studied using the Z-scan measurement and a much enhanced nonlinear optical performance was observed compared with that of the benchmark material-C$_{60}$ and graphene. This may be partially attributed to the photoinduced electron transfer mechanism between graphene and C$_{60}$.

Keywords: Graphene Oxide, Fullerenol, Graphene-C$_{60}$, Nonlinear Optical.

1. INTRODUCTION

Graphene, an atomically thin sheet of carbon atoms tightly packed in a two-dimensional (2D) honeycomb lattice, has attracted great interest in recent years due to its unique physical properties.[1] Such unique properties and bulk availability at high purity make it a realistic candidate for a number of technological applications, such as field–effect transistors,[2] resonators,[3] transparent anode,[4] etc. In the meantime, other allotropic carbon nanomaterials, such as fullerenes, have been studied intensively in the last decade for their potential applications due to their photoconducting, superconductivity and nonlinear optical (NLO) properties, etc.[5] The last asset, due to fullerene's higher triplet–triplet absorption cross sections than the ground-state absorption cross sections,[6] could led to numerous applications in laser protecting devices, telecommunication systems and other optical signal processing applications. Also, to enhance their NLO performance, various functionalized fullerenes have been made and studied.[6–8] For example, Tang et al.[7] described a Poly(1-phenyl-1-alkynes)-bound C$_{60}$ and demonstrated that this polymer improved the NLO performance of the C$_{60}$ solution. Liu and co-workers[8] reported that the C$_{60}$ organophosphorus derivatives showed a larger optical nonlinearities than

C$_{60}$, thus improving the properties of fullerene. Due to its unique and large 2D π-electron conjugation systems, much like that in C$_{60}$ and carbon nanotubes (CNTs), we expect that the hybrid combining graphene and fullerene would feature not only the intrinsic properties of individual graphene and fullerene, but in some circumstances new behavior and functions arising from the mutual π interaction between graphene and fullerene, and an enhanced NLO behavior than C$_{60}$ and graphene may be generated.

In this paper, we report the synthesis of the graphene-C$_{60}$ hybrid and its NLO property. The graphene-C$_{60}$ hybrid material was investigated using spectroscopic methods and thermal gravimetric analysis (TGA). The NLO performance of this hybrid material was studied using the Z-scan measurement with linearly polarized 5 ns pulses at 532 nm. And a much enhanced NLO result was observed compared with that of benchmark material-C$_{60}$ and graphene.

2. EXPERIMENTAL DETAILS

2.1. Instruments and Measurements

Fourier transform infrared spectroscopy (FTIR) spectra were obtained on a BRUKER Tensor 27 spectrometer. The samples were homogeneous dispersed in KBr pellets.

UV-Vis spectra were performed on a JASCO V-570 spectrometer. Raman spectra were measured by a Renishaw inVia Raman microscope at room temperature with the 514 nm line of an Ar ion laser as an excitation source. Thermal gravimetric analysis (TGA) curves were recorded on a NETZSCH STA 409PC instrument under purified nitrogen gas flow with a 5 °C/min heating rate. Atomic force microscopy (AFM) studies were performed using a Digital Instruments Dimension 3100 in the tapping mode. Elemental analysis (EA) was performed on a Yanaca CDRDER MT-3 instrument.

The nonlinear optical and Z-scan experiments were preformed with linearly polarized 5 ns pulses at 532 nm generated from a frequency doubled Q-switched Nd:YAG laser. The spatial profiles of the pulses were of nearly Gaussian distribution after the spatial filter. The pulse was divided by a beam splitter into two parts. The reflected part was taken as the reference representing the incident light energy and the transmitted beam was focused through the sample. Both the incident and transmitted pulse energies were monitored simultaneously by two energy detectors (Molectron J3S-10). The sample was mounted on a translation stage, moving along the Z-axis with respect to the focal point. By keeping the incident pulse energy constant at 41.5 mJ, the light transmission through the sample was measured with respect to the sample Z-position. The samples were placed in quartz cells with 1 mm thickness, which were placed at the focus of a lens with a focal length of 250 mm.

2.2. Synthesis of Graphene Oxide (GO)

GO was prepared according to a modified hummers method.[9] The GO was confirmed to exist as individual sheets in solution.[10] The sizes of the GO sheet are mainly distributed between 200 and 500 nm determined by a statistical analysis using atomic force microscopy (AFM, see Fig. 1). In detail, graphite powder (5 g), NaNO$_3$ (3.75 g) and KMnO$_4$ (15 g) was vigorously stirred at room temperature for 5 days in concentrated H$_2$SO$_4$ (375 ml). After that 5% H$_2$SO$_4$ (1 L) aqueous solution was added to the reaction with the temperature kept at 98 °C for 2 h. Then the reaction was cooled to 60 °C. After 30% H$_2$O$_2$ (30 ml) was added and the reaction was further stirred for another
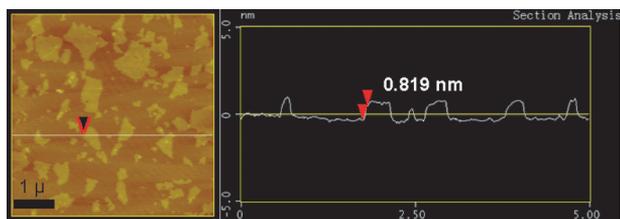

Fig. 1. AFM image of graphene oxide (GO). The sample was prepared by spin coating (2000 rpm, 30 s) GO solution (0.2 mg/mL) in H$_2$O on a mica surface.

2 h, the mixture was centrifuged to collect the bottom product and sequently washed with 5% H$_2$SO$_4$/0.5% H$_2$O$_2$ (10 times), 5% HCl solution (5 times), and then washed repeatedly with water until the pH of the supernatant was neutral. Finally the material was dried to obtain a loose brown powder (EA: C:H:O = 45.72:3.28:51.00).

2.3. Synthesis of Fullerenol

Fullerenol was synthesized following the literature procedure[11] and the average composition of the fullerenol was C$_{60}$(OH)$_5$ determined by elemental analysis (C:H:O = 85.47:0.57:13.96).
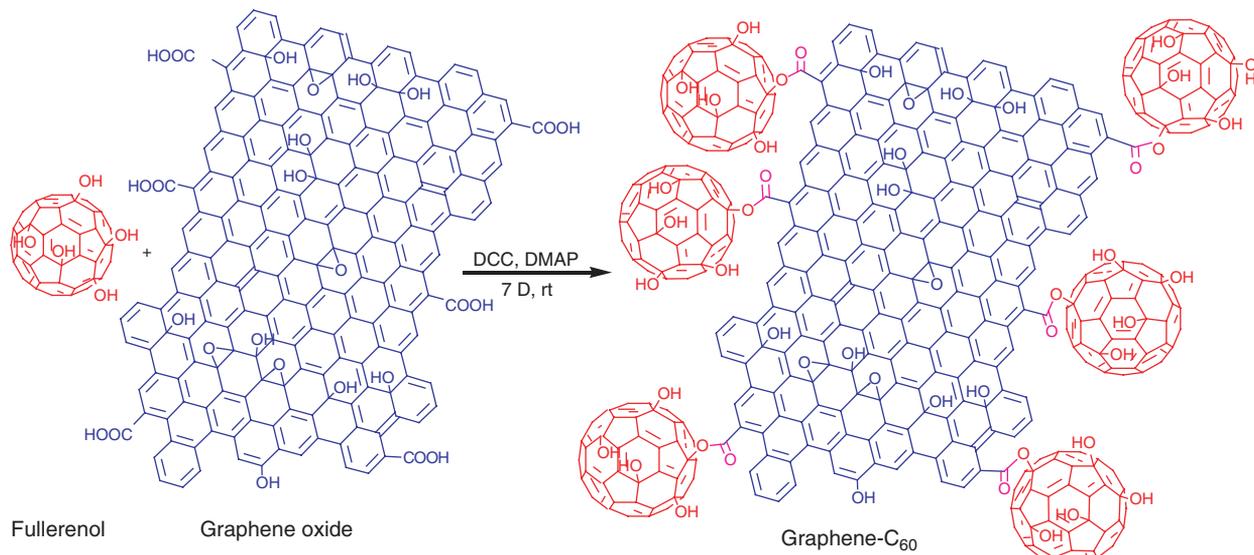
2.4. Synthesis of the Graphene-C$_{60}$ Hybrid

The graphene-C$_{60}$ hybrid was prepared by a simple condensation reaction between graphene oxide (GO)[9, 10] and fullerenol.[11] The synthesis procedure for the graphene-C$_{60}$ hybrid is shown in Scheme 1, using a mild coupling reaction between –OH group of fullerenol and –COOH group of GO.[12] In detail, GO (50 mg), fullerenol (55 mg), 1,3-dicyclohexylcarbodiimide (DCC) (32 mg) and 4-(dimethylamino)-pyridine (DMAP) (2 mg) were added into anhydrous *N*,*N*-dimethyl-formamide (DMF) (40 ml). The solution was purged with Ar and stirred for 7 days in dark at room temperature. On completion of the reaction, the solution was centrifuged and washed with DMF for several times until the unreacted fullerenol was completely removed (monitored by thin layer chromatography). Finally the deposition was washed with acetone and dried under vacuum to obtain the graphene-C$_{60}$ hybrid product (72 mg) (EA: C:H:O = 57.64:1.82:40.54). The upper combined supernate solution from this workup was then used to measure the unreacted fullerenol (see Fig. 2).

3. RESULTS AND DISCUSSION

3.1. Determination the Content of C$_{60}$ in the Graphene-C$_{60}$ Hybrid

In order to calculate the content of C$_{60}$ in the graphene-C$_{60}$, we used the UV method to measure the unreacted fullerenol concentration in the centrifuge supernate during the workup of the reaction. As the fullerenol has a good solubility in DMF, it should obey the Lambert-Beer's law (see Fig. 2). On the basis of Lambert-Beer's law, we estimated the concentration of the unreacted fullerenol in the supernate to be 0.348 mg/ml (the supernate was diluted ten times before the UV measurement), and the amount of unreacted fullerenol to be 37.6 mg. Thus, the weight fraction of C$_{60}$ in the graphene-C$_{60}$ hybrid material was estimated to be ~24.2% (graphene:C$_{60}$ = 3:1, weight ratio). Combing the result of EA measurement, it was estimated that one C$_{60}$ molecule is covalently attached for every ~110 carbon atoms in the graphene.

Scheme 1. Synthesis procedure of the graphene-C$_{60}$ hybrid.

3.2. Characterization of the Graphene-C$_{60}$ Hybrid

Figure 3(a) shows the Fourier transform infrared spectroscopy (FTIR) of GO, fullerenol and the graphene-C$_{60}$ hybrid. The notable feature of GO is the absorption band corresponding to the carboxyl stretching mode at 1730 cm^{-1}. Comparing with GO, the graphene-C$_{60}$ reveals a new peak at 1717 cm^{-1}, which can be attributed to the ester group.[13] This strongly suggests that C$_{60}$ has been chemically attached to the graphene sheet by the ester bond. We also performed the Raman spectroscopy of

GO, fullerenol and the graphene-C$_{60}$ hybrid, as shown in Figure 3(b). The GO spectrum shows an intense tangential mode (G band) at 1599 cm^{-1}, with a disordered-induced peak (D band) at 1354 cm^{-1}.[14] The spectrum of fullerenol reveals two peaks at 1375 and 1594 cm^{-1}, respectively. The graphene-C$_{60}$ shows two peaks at 1368 (D band) and 1589 cm^{-1} (G band). Comparing with GO, the graphene-C$_{60}$ hybrid shows a 14 cm^{-1} up-shift for the D band and 10 cm^{-1} down-shift for the G band in its spectrum. These considerable shifts should be caused by the strong interaction between C$_{60}$ and graphene.[15]

The TGA curves of GO, fullerenol, the graphene-C$_{60}$ hybrid and GO/fullerenol blend (controlled sample) are shown in Figure 4. The curve pattern of the controlled sample is similar to GO before 225 °C, while after that it follows the graphene-C$_{60}$ hybrid. These results provide further evidence for the covalent linkage between graphene and C$_{60}$.

3.3. Nonlinear Optical Performance of the Graphene-C$_{60}$ Hybrid

We carried out the open-aperture Z-scan[16] experiments to investigate the NLO performance of GO, graphene-C$_{60}$, fullerenol, GO/fullerenol blend and C$_{60}$ with the same concentration of 0.1 mg/ml, as shown in Figure 5. The incident single-pulse energy of the source was about 41.5 μJ. The samples were placed in quartz cells with 1 mm thickness, which were placed at the focus of a lens with a focal length of 250 mm, and C$_{60}$ was employed as a benchmark material. When the Z-position was 'far' away from the focal point, which means low input fluence, all the materials exhibit linear optical behaviors. However, at focal point where the input fluence is maximum, the transmittances of GO, graphene-C$_{60}$, GO/fullerenol blend, fullerenol and C$_{60}$
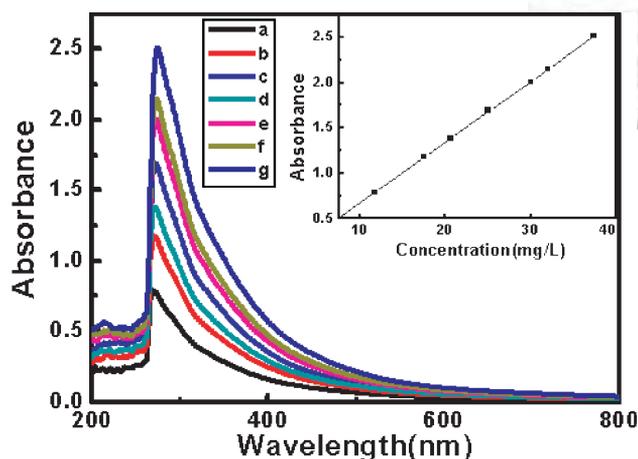

Fig. 2. Concentration dependence of UV absorption of fullerenol in DMF, prepared with the standard concentrations of 12, 17, 21, 25, 30, 32, 37 mg/L for fullerenol (from *a* to *g*, respectively). The inset is the plot of the absorption (at 271 nm) of fullerenol versus concentration. The straight line was a linear least-square fit to the data to be 0.067 L mg^{-1} cm^{-1} with an *R* value of 0.999, which indicates the fullerenol was dissolved homogeneously in the solvent. This plot was then used to calculate the concentration of the unreacted fullerenol and further for the content of C$_{60}$ in the graphene-C$_{60}$ hybrid.
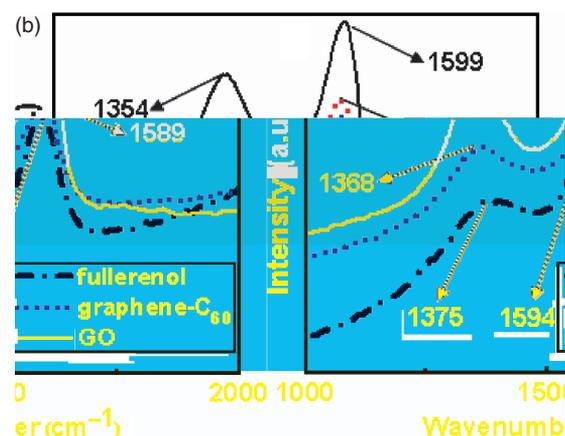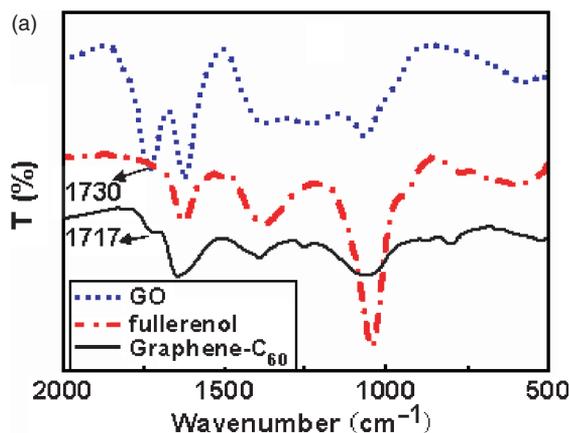
Fig. 3. (a) FTIR of GO (dotted line), fullerenol (dash dot line) and graphene-C_{60} (solid line). The disappearance of the –COOH group at 1730 cm^{-1} and the formation of the ester group at 1717 cm^{-1} in the graphene-C_{60} indicate that C_{60} has been chemically attached to graphene. (b) Raman spectroscopy of GO (solid line), fullerenol (dash dot line) and graphene-C_{60} (dotted line). Comparing with GO, the graphene-C_{60} shows 14 cm^{-1} up-shift for the D band and 10 cm^{-1} down-shift for the G band. These considerable shifts should be caused by the strong interaction between C_{60} and graphene.
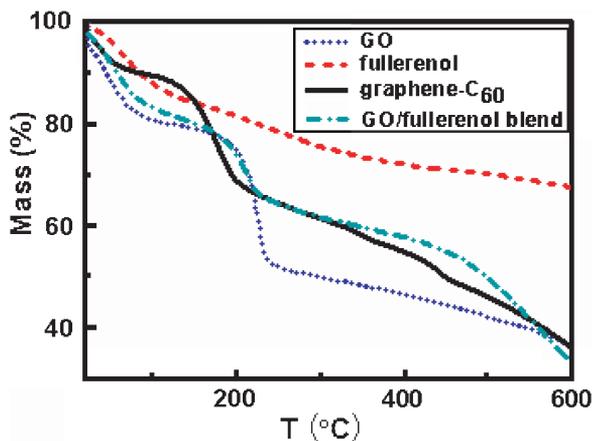

Fig. 4. TGA of GO (dotted line), fullerenol (dashed line), graphene-C_{60} (solid line) and GO/fullerenol mixture (dash dot line). All the samples were running under purified nitrogen gas flow with a 5 °C/min heating rate.
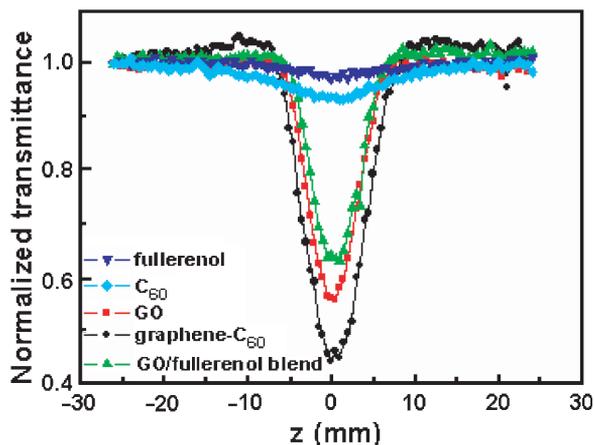

Fig. 5. Open aperture Z-scan results of GO (■), graphene-C_{60} (●), GO/fullerenol blend (▲), fullerenol (▼) in DMF and C_{60} (♦) in toluene with the same concentration of 0.1 mg/ml for 5 ns pulsed laser at 532 nm. The graphene-C_{60} has the largest dip among the transmittance curves of these materials, indicating that it has the best NLO effect.

drop down to 44.3%, 34.3%, 52.4%, 87.8%, and 83.9%, respectively. These results demonstrate that while excellent nonlinear optical performance of all the samples were observed, the larges dip among the transmittance curves indicates that the graphene-C_{60} hybrid has the best nonlinear optical effort.[17] Different mechanisms exist for NLO, such as nonlinear absorption, nonlinear refraction, and nonlinear light scattering. The NLO property of C_{60} comes from the conjugative effect of C_{60} molecule, according to reverse saturable absorption mechanism.[18] Carbon nanotube suspensions have also been reported to have strong nonlinear optical effects, which arise from strong nonlinear light scatterings due to the creation of new scattering centers consisting of ionized carbon microplasmas and solvent microbubbles.[19] The reason for the graphene-C_{60} hybrid showing the best NLO performance is yet to be understood. But from the similar electronic structure of C_{60}, graphene and CNTs, it is reasonable to expect that both nonlinear absorption and nonlinear light scattering mechanism may play a role for the enhanced NLO performance of the hybrid. Actually, during the measuring process, GO, graphene-C_{60} hybrid and GO/fullerenol blend all showed obvious nonlinear scattering signal, which may be assigned to the incandescence and submission of graphitic particles leading to the fast growth of hot carbon vapor bubble, similar to the mechanism of CNTs.[19] Another possible reason for the enhanced NLO performance of graphene-C_{60} hybrid may be attributed to the possible photoinduced electron transfer mechanism (similar to the carbon nanotubes-C_{60} system[20]) between graphene and C_{60}, as observed in the PVK-modified SWCNTs system.[21]

4. CONCLUSION

In conclusion, the graphene-C_{60} hybrid material has been synthesized by a simple condensation reaction and fully

characterized. The covalent linkage between graphene and C$_{60}$ has been confirmed by FTIR and TGA. Raman spectroscopy suggested a strong interaction between the C$_{60}$ cage and graphene sheet. Its enhanced NLO performance than its parent species C$_{60}$ and graphene may be attributed at least partially to the photoinduced electron transfer mechanism between the graphene sheet and C$_{60}$. Further studies to understand better the mechanism and the structure-property correlations are currently underway.

References and Notes

1. A. K. Geim, and K. S. Novoselov, *Nat. Mater.* 6, 183 (**2007**).
2. X. L. Li, X. R. Wang, L. Zhang, S. W. Lee, and H. J. Dai, *Science* 319, 1229 (**2008**).
3. J. S. Bunch, A. M. van der Zande, S. S. Verbridge, I. W. Frank, D. M. Tanenbaum, J. M. Parpia, H. G. Craighead, and P. L. Mceuen, *Science* 315, 490 (**2007**).
4. X. Wang, L. Zhi, and K. Müllen, *Nano Lett.* 8, 323 (**2008**).
5. F. Wudl, *J. Mater. Chem.* 12, 1959 (**2002**).
6. Y. P. Sun, G. E. Lawson, J. E. Riggs, B. Ma, N. X. Wang, and D. K. Moton, *J. Phys. Chem. A* 102, 5520 (**1998**).
7. B. Z. Tang, H. Y. Xu, J. W. Y. Lam, P. P. S. Lee, K. T. Xu, Q. H. Sun, and K. K. L. Cheuk, *Chem. Mater.* 12, 1446 (**2000**).
8. Z. B. Liu, J. G. Tian, W. P. Zang, W. Y. Zhou, C. P. Zhang, J. Y. Zheng, Y. C. Zhou, and H. Xu, *Appl. Opt.* 42, 7072 (**2003**).
9. W. S. Hummers and R. E. Offeman, *J. Am. Chem. Soc.* 80, 1339 (**1958**).
10. H. A. Becerril, J. Mao, Z. F. Liu, R. M. Stoltenberg, Z. N. Bao, and Y. S. Chen, *ACS Nano* 2, 463 (**2008**).
11. L. Y. Chiang, L. Y. Wang, J. W. Swirczewski, S. Soled, and S. Cameron, *J. Org. Chem.* 59, 3960 (**1994**).
12. Y. Lin, B. Zhou, K. A. S. Fernando, P. Liu, L. F. Allard, and Y. P. Sun, *Macromolecules* 36, 7199 (**2003**).
13. M. Alvaro, P. Atienzar, P. de la Cruz, J. L. Delgado, H. Garcia, and F. Langa, *Chem. Phys. Lett.* 386, 342 (**2004**).
14. C. Gomez-Navarro, R. T. Weitz, A. M. Bittner, M. Scolari, A. Mews, M. Burghard, and K. Kern, *Nano Lett.* 7, 3499 (**2007**).
15. J. L. Delgado, P. de la Cruz, A. Urbina, J. T. López Navarrte, J. Casado, and F. Langa, *Carbon* 45, 2250 (**2007**).
16. M. Sheik-Bahae, A. A. Said, T. H. Wei, D. J. Hagan, and E. W. Van Stryland, *IEEE J. Quantum Electron.* 26, 760 (**1990**).
17. Z. B. Liu, J. G. Tian, Z. Guo, D. M. Ren, F. Du, J. Y. Zheng, and Y. S. Chen, *Adv. Mater.* 20, 511 (**2008**).
18. S. R. Mishra, H. S. Rawat, and S. C. Mehendale, *Appl. Phys. Lett.* 71, 46 (**1997**).
19. J. E. Riggs, D. B. Walker, D. L. Carroll, and Y. P. Sun, *J. Phys. Chem. B* 104, 7071 (**2000**).
20. W. Wu, H. R. Zhu, L. Z. Fan, and S. H. Yang, *Chem. Eur. J.* 14, 5981 (**2008**).
21. W. Wu, S. Zhang, Y. Li, J. X. Li, L. Q. Liu, Y. J. Qin, Z. X. Guo, L. M. Dai, C. Ye, and D. B. Zhu, *Macromolecules* 36, 6286 (**2003**).